List of Errata

(2024 IEEJ, Annual Conference of PE)

Note; this first page indicated 8–6–17 page.

Position	Before Correction	After Correction
Second page, left, Eq. (5).	$\psi_{c0} = k_\psi \varepsilon_0$	$\psi_{c0} = \frac{1}{k_\psi \varepsilon_0}$
Second page, left, 12th and 13th lines from the bottom.	amplitudes $A_{IR\text{-}ori}$, as shown in Eqs. (11) and (12). $c\rho$ and $\psi'_{c0\text{-}ap}$ of τ are determined using β_{ir}.	amplitudes $A_{IR\text{-}ori}$ and influenced on $\lambda'_c + \lambda'_r$ (Eqs. (11) and (12)).
Second page, left, Eqs. (10) – (12).	$\Delta IR_{ori} = 6{A_{IR-ori}}^2 v_{eigen} v$ $\left(IR_{ori} = {A_{IR-ori}}^2 {v_T}^2, \Delta V = 1\right)$ (10) $\beta_{ir} = \frac{3h'm(1-\lambda'_c-\lambda'_r)}{16\pi^4 r_1^6 M {A_i}^2 v_{eigen} k_\psi \varepsilon_0} = \frac{{A_{IR-ori}}^2}{2\pi^2 M {A_i}^2}$ (11) $A_{IR-ori} = \sqrt{\frac{h'c\rho}{6\tau v_{eigen}}}$ (12)	$\Delta IR_{ori} = 12\pi^2 k_{Aq}^2 q^2 {A_{IR-ori}}^2 v_{eigen} v$ $\left(IR_{ori} = 6\pi^2 k_{Aq}^2 q^2 {A_{IR-ori}}^2 {v_T}^2, V = 1\right)$ (10) $\beta_{ir} = \frac{3h'm(1-\lambda'_c-\lambda'_r)}{16\pi^4 r_1^6 M {A_i}^2 v_{eigen} \psi_{c0}} = \frac{\Delta IR_{ori}}{\Delta E} = \frac{k_{Aq}^2 q^2 {A_{IR-ori}}^2}{A_i^2 M}$ (11) $A_{IR-ori} = \frac{1}{2\pi}\sqrt{\frac{h'c\rho}{3\tau v_{eigen}}} = \frac{1}{4\pi^2 r_1^3 k_{Aq} q}\sqrt{\frac{3mh' k_\psi \varepsilon_0 (1-\lambda'_c-\lambda'_r)}{v_{eigen}}}$ (12)
Third page, right, the label of vertical axis in Fig. 6 (b).	Δ Ai / Aeigen, P' / P'eigen (10^5m)	Δ Ai / Aeigen, P' / P'eigen
Third page, right, 13th line from the bottom.	Ions N_{re} accepted large P', retaining vibration states	Ions N_{re} accepted large P' and became standby release ions retaining vibration states

<table>
<tr><th>Position</th><th>Before Correction</th><th>After Correction</th></tr>
<tr><td>Fourth page, right, legend in Fig.12.</td><td>Φ OH-before</td><td>Φ OH-after</td></tr>
<tr><td>Fourth page, right, Fig.11 and Fig.13.</td><td>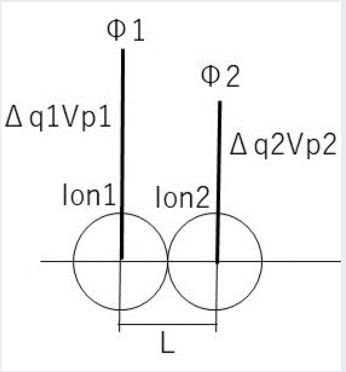

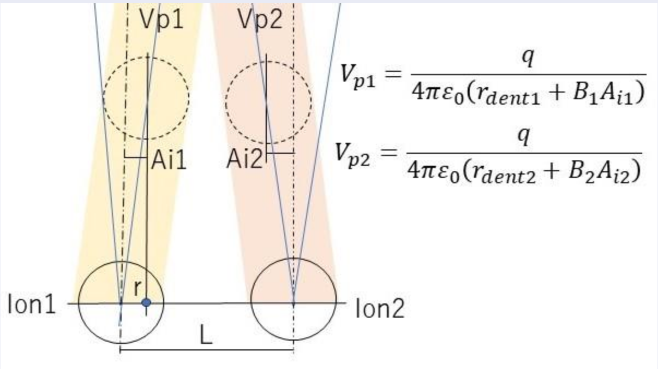
</td><td>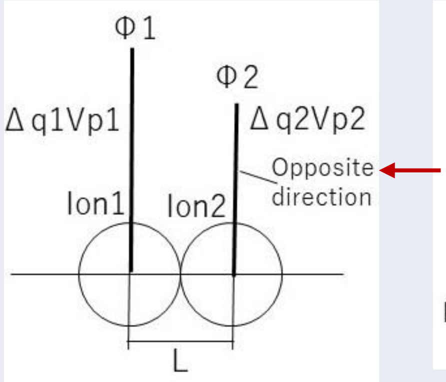

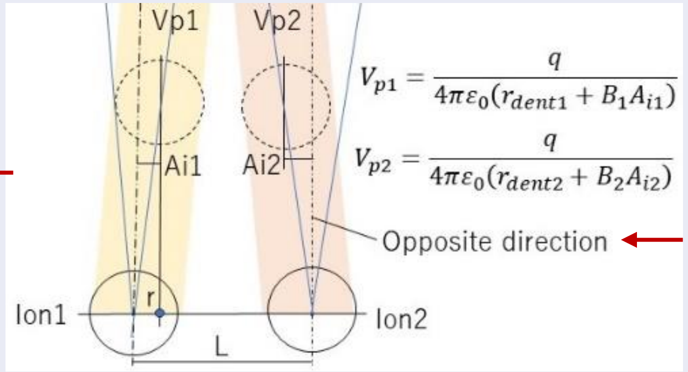
</td></tr>
<tr><td>Fifth page, left, 16th – 19th line from the top.</td><td>Ion spins were generated by the unbalanced location of electrical charge because ion comprised elementary particles, at the same time as ion SHM, referencing Section 2.2 of the paper (2). First, as mentioned in Section 7.2, the SHM of a released ion was influenced by ion spins alone, and its A_i was prevented by spins. ・・・. Next, spin radii r_t was fixed, and the ω of spins resonated with the v_T of SHM.</td><td>Ion spins were generated by the unbalanced location of electrical charge because ion comprised elementary particles, at the same time as ion SHM. Ion spins comprising two axes in 3D motion received and emitted IR energy, referencing Section 2.2 of the paper (2). First, as mentioned in Section 7.2, the SHM of a released ion was influenced by ion spins alone, and its A_i was prevented by spins. ・・・. Next, spin radius r_t was fixed, and the ω of spins resonated with the v_T of SHM.</td></tr>
<tr><td>Sixth page, right, legend in Fig.22.</td><td>rdent=1.38*10^-9m
Aeigen=3.66*10^-12m
veigen=1.85*10^13Hz
B=10000, Limited γ r=1.117</td><td>rdent-after=1.38*10^-9m
Aeigen=3.66*10^-12m
veigen=1.85*10^13Hz
B=10000, Limited γ r=1.117</td></tr>
</table>

Position	Before Correction	After Correction
Seventh page, right, 8.3. Invisible energy of Ai preventions.	The A_i prevention energy was denoted as ΔE_{preAi} that energy transfer from a portion of ΔE_{other} to ΔE_{SHM} was used in the simulations. However, ΔE_{preAi} was not actually present (Eq. (75)). ・・・. Hence, because of the application of the same SHM equation, energy transfer did not occur. $\Delta E_{SHM} = P' - \Delta E_{other}$ $\left(\Delta E_{pre\ Ai} = E_{SHM-after} - E_{SHM} = 0\right)$ $= \frac{3}{2} M\omega^2 v_T^2 \left((A_i + \Delta A_i)^2 - {A_i}^2\right) - \Delta E_{other0}$ $= \frac{3}{2} M\omega^2 A_i^2 \left((v_T + \Delta v_T)^2 - v_T^2\right) + \Delta E_{preAi} - \Delta E_{other0}$ (75)	The A_i prevention energy was denoted as ΔE_{preAi}, which was not actually present (Eq. (75)). ・・・. The subscripts "atΔA_i" and "atΔv_T" denote ΔE_{other0} before and after prevention A_i. $\Delta E_{pre\ Ai} = E_{SHM-after} - E_{SHM}$ $\left(\omega_{eigen} = 2\pi v_{eigen}\right)$ $P' = \frac{3M\omega_{eigen}^2\left((A_{eigen}+\Delta A_i)^2 - A_{eigen}^2\right)}{2} + \Delta E_{other0-at\Delta A_i} - \Delta E_{pre\ Ai}$ $= \frac{3}{2} M A_{eigen}^2 \left((\omega_{eigen} + \Delta\omega)^2 - \omega_{eigen}^2\right) + \Delta E_{other0-at\Delta v_T}$ (75)
Eighth page, left, 1th line from bottom.	Every time the phase changes, the initial value A_{oth0} varies.	(Elimination)
Eighth page, Figs. 24–(a), 26, 29, and 30.	ΔEother2 and lnΔEother2.	ΔEother and lnΔEother. ("2" was eliminated)
Ninth page, left, 3th line from the top.	The number of resonating ions N_{rs} gradually increased with T until N_T at about 120℃.	The number of resonating ions N_{rs} gradually increased with T until N_T at about 120 – 500℃.
Ninth page, left, 25th – 30th lines from the top.	For $T < 273$ K, c was approximately equal to c_1 because N_{rs} was small; hence, $k_{\omega r} = k_{\omega f} = k_\omega \propto N_{rs}/N_T$ was smaller than that at $T \geq 273$ K. Here, the probability of generating resonating ions was small. Ions did not possess sufficient kinetic energy to increase with the quadratic equation.	At $393 \leq T < 773$ K, the high slope property of $c - T$ is depicted in Fig. 28. ΔE_{other} influenced c because exponents of ΔE_{SHM} in ΔE_{other} increased from 1 to 2. $k_{\omega r} = k_{\omega f} = k_\omega \propto N_{rs}/N_T$ was smaller than k_ω=1 at $T \geq 773$ K. Here, the probability $p_{r\text{-}rs}$ of generating resonating molecules was under 1. For $T < 273$ K, N_{rs} was small. c was approximately equal to c_1 because ions did not possess sufficient kinetic energy to increase with the quadratic equation.

Position	Before Correction	After Correction
Ninth page, left – right, 5th – 4th lines from the bottom and top, respectively.	Therefore, according to the curve trend observed in Fig.34, resonation probability $p_{r\text{-}rs}$ in Eq. (86) was derived (Fig. 35). Hence, $N_{rs} = N_T p_{r-rs} \approx N_T\, T/T_c$. p_{r-rs} property was almost straight line and affected by A_{oth0} size to result from T_c proportional to $k_{T-base} - k_T\|_{P'=P'c}$, where $A_{oth0} = A_{eigen}/10$ at $T_c = 393\,K$ was assumed. At $T < 393\,K$, owing to $\Delta\omega$ from small N_{rs}, ΔE_{other} was expressed as linear equation ΔE_{other1} because ΔE_{other2} was omitted by low T (Fig. 30 and Eq. 87).	Therefore, according to the curve trend observed in Fig.34, $p_{r\text{-}rs}$ was derived from ζ_{pr} (Eq. (86) and Fig. 35). Hence, $N_{rs} = N_T p_{r-rs} \approx N_T\, T/T_c$. ζ_{pr} property was affected by A_{oth0} size, with which $p_{r\text{-}rs}$ varied from a steady $\zeta_{pr}\|_{T=Tc}$. T_c and $P'\|_{T=Tc}$ were proportional to A_{oth0} and $1/\zeta_{pr}\|_{T=Tc}$. At $T < 393\,K$, owing to small P', ΔE_{other} was expressed as linear equation ΔE_{other1} because ΔE_{other2} was omitted by $E_{other0} \gg \Delta E_{other}$ (Fig. 30 and Eq. (87)). Consequently, the follow-up ability ζ_{pr} slightly and uniformly appeared, with $p_{r-rs} \approx 0.006$, as determined from comparison of ΔE_{other} at 500℃ in Figs. 36 and 37.
Ninth page, right, Figs. 34 and 35.	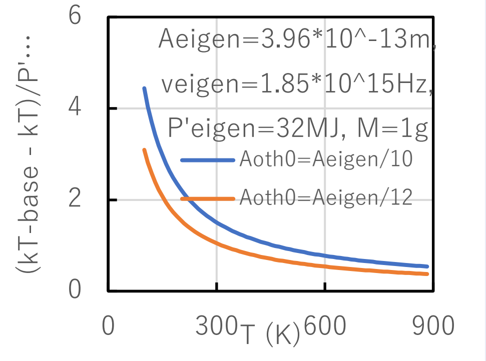 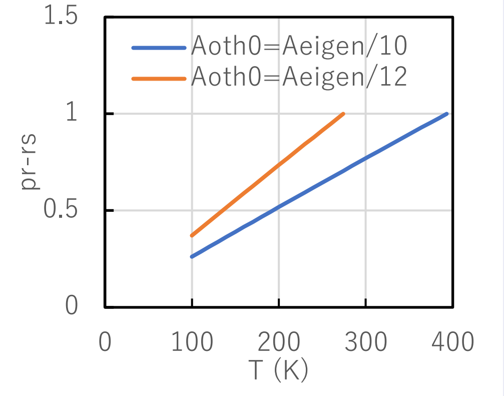	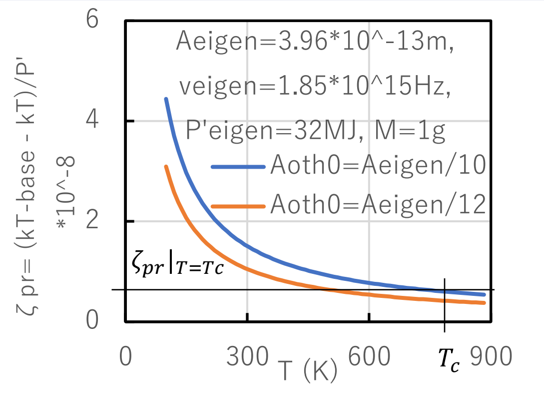 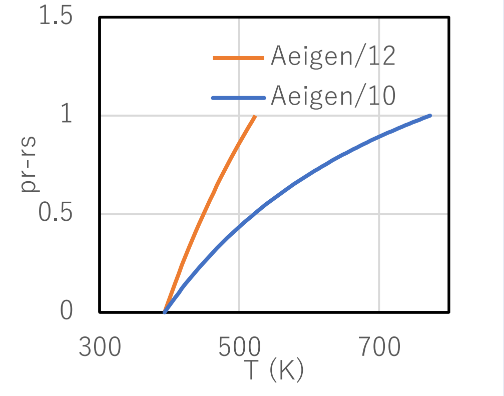
Ninth page, right, Eq. (86)	$p_{r-rs} = \frac{\zeta_{pr}\|_{P'=P'c}}{k_{T-base}-k_T} P'(0 < P' \le P'_c, P' = P'_c\ at\ T = T_c)$ (86)	$p_{r-rs} = \frac{\zeta_{pr}-\zeta_{pr}\|_{T=120^\circ C}}{\zeta_{pr}\|_{T=Tc}-\zeta_{pr}\|_{T=120^\circ C}}\ (Tc = 500^\circ C)$ $\left(\frac{P'_{eigen}}{P'\|_{T=Tc}} = \eta\frac{A_{eigen}^{2}}{A_{otho}^2} + \eta - 1, \eta = \frac{3A_{eigen}^{2}\zeta_{pr}\|_{T=Tc}}{2}\right)$ (86)

Position	Before Correction	After Correction
10th page, left, legends in Figs.42 and 43.	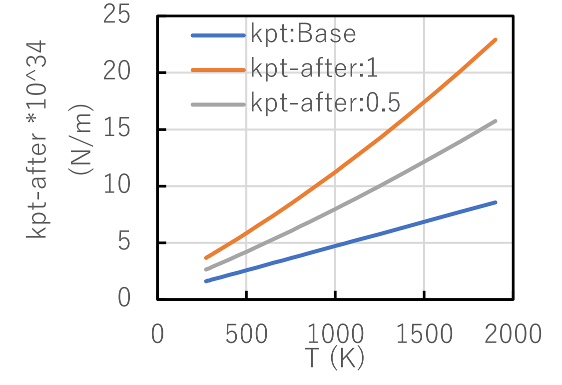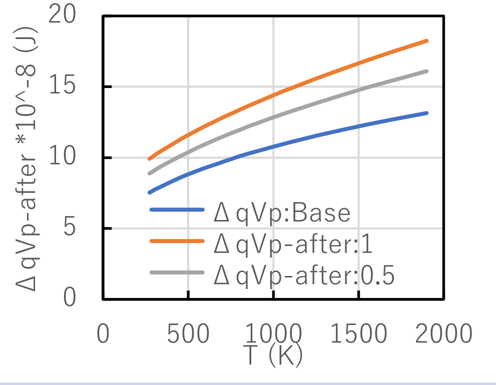	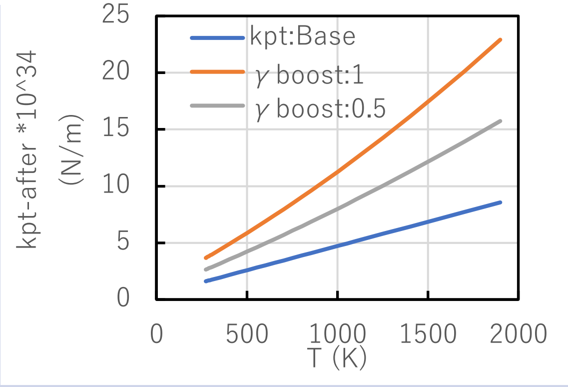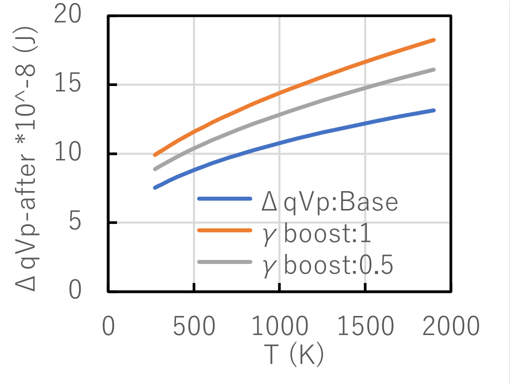
11th page, left, Eqs. (103) – (107).	$E_{IR} = \frac{3V}{2} A_{IR}^2 v_T^2 = \frac{3V}{2} A_{IR-limit}^2 v_{Tmax}^2$ (103) $\Delta E_{IR} = \frac{3VA_{IR}^2(v_T^2 - v_{eigen}^2)}{2}$ $\approx 3VA_{IR}^2 v_{eigen} v \approx 3VA_{IR-limit}^2 v_{eigen} v_{max}$ $\left(p' \approx 3A_{IR-limit}^2 v_{eigen} v_{max}, P'_{eigen} = \frac{3VA_{IR}^2 v_{eigen}^2}{2}\right)$ (104) $\Delta P'_{n'} = 3\Delta V_{n'} A_{IR}^2 (v_{Tn'}^2 - v_{eigen}^2)$ $\approx 6\Delta V_{n'} A_{IR}^2 v_{eigen} \Delta v_{Tn'}$ (105) $\Delta P'_{unit-n'} = 3\Delta V_{n'} A_{IR}^2 \left((v + v_{eigen})^2 - v_{eigen}^2\right)$ $\approx 6\Delta V_{n'} A_{IR}^2 v_{eigen} v$ (106) $A_{IR-limit} = \frac{1}{V}\sqrt{\frac{mh\prime}{3\psi\prime_{c0-\alpha p} v_{eigen}}}$ $(\Delta P'_{unit-n'} \approx 6\Delta V_{n'} A_{IR-limit}^2 v_{eigen} v_{max},)$ (107)	$E_{IR} = 3\pi^2 k_{Aq}^2 q^2 V A_{IR}^2 v_T^2 = 3\pi^2 k_{Aq}^2 q^2 V A_{IR-limit}^2 v_{Tmax}^2$ (103) $\Delta E_{IR} = 3\pi^2 k_{Aq}^2 q^2 V A_{IR}^2 (v_T^2 - v_{eigen}^2)$ $\approx 6\pi^2 k_{Aq}^2 q^2 V A_{IR}^2 v_{eigen} v \approx 6\pi^2 k_{Aq}^2 q^2 V A_{IR-limit}^2 v_{eigen} v_{max}$ $(P'_{eigen} = 3\pi^2 k_{Aq}^2 q^2 V A_{IR}^2 v_{eigen}^2)$ (104) $\Delta P'_{n'} = 6\pi^2 k_{Aq}^2 q^2 \Delta V_{n'} A_{IR}^2 (v_{Tn'}^2 - v_{eigen}^2)$ $\approx 12\pi^2 k_{Aq}^2 q^2 \Delta V_{n'} A_{IR}^2 v_{eigen} \Delta v_{Tn'}$ (105) $\Delta P'_{unit-n'} = 6\pi^2 k_{Aq}^2 q^2 \Delta V_{n'} A_{IR}^2 \left((v + v_{eigen})^2 - v_{eigen}^2\right)$ $\approx 12\pi^2 k_{Aq}^2 q^2 \Delta V_{n'} A_{IR}^2 v_{eigen} v$ (106) $A_{IR-limit} = \sqrt{1.5} K_A$ $(\Delta P'_{unit-n'} \approx 12\pi^2 k_{Aq}^2 q^2 \Delta V_{n'} A_{IR-limit}^2 v_{eigen} v_{max},)$ (107)

Position	Before Correction	After Correction
11th page, left, Eqs.(108) – (110).	$A_{IR} = \frac{3}{4\pi r_1^3}\sqrt{\frac{mh\prime\sqrt{n\prime}}{3\psi\prime_{c0-ap}v_{eigen}}\left(\frac{4m^{1.5}-6m\sqrt{n\prime}+2n\prime^{1.5}}{3(m-n\prime)(1-e^{-t/\tau})}\right)}$ $= K_A\sqrt{2\sqrt{n'}\left(\frac{2m^{1.5}-3m\sqrt{n\prime}+n\prime^{1.5}}{3(m-n\prime)(1-e^{-t/\tau})}\right)}$ $\begin{pmatrix} P_{flow,n\prime} \approx 6A_{IR}^2 v_{eigen}\Delta v_{Tn'}\Delta V_{n'}, \\ K_A = \frac{3}{4\pi r_1^3}\sqrt{\frac{mh\prime}{3\psi\prime_{c0-ap}v_{eigen}}} \end{pmatrix}$ (108) $A_{IR-ori} = \frac{3}{4\pi r_1^3}\sqrt{\frac{2mn\prime h\prime}{3\psi\prime_{c0-ap}v_{eigen}}} = K_A\sqrt{2n'}$ $(IR_{ori,n\prime} \approx 6A_{IR-W}^2 v_{eigen}\Delta v_{Tn'}\Delta V_{n'})$ (109) $(IR_{total,n\prime} \approx 6A_{IR-total}^2 v_{eigen}\Delta v_{Tn'}\Delta V_{n'})$ (110)	$A_{IR} = \sqrt{\frac{2m^{1.5}\sqrt{n\prime}-3mn\prime+n\prime^2}{(m-n')(1-e^{-t/\tau})}}K_A$ $\begin{pmatrix} P_{flow,n\prime} \approx 12\pi^2 k_{Aq}^2 q^2 A_{IR}^2 v_{eigen}\Delta v_{Tn'}\Delta V_{n'}, \\ K_A = \frac{1}{4\pi^2 r_1^3 k_{Aq} q}\sqrt{\frac{2mh'k_\psi\varepsilon_0(1-\lambda\prime_c-\lambda\prime_r)}{v_{eigen}}} \end{pmatrix}$ (108) $A_{IR-ori} = \sqrt{3n'}K_A$ $(IR_{ori,n\prime} \approx 12\pi^2 k_{Aq}^2 q^2 A_{IR-ori}^2 v_{eigen}\Delta v_{Tn'}\Delta V_{n'})$ (109) $(IR_{total,n\prime} \approx 12\pi^2 k_{Aq}^2 q^2 A_{IR-total}^2 v_{eigen}\Delta v_{Tn'}\Delta V_{n'})$ (110)
11th page, left, 5th – 9th lines from the bottom.	Thus, $p' = 2A_{IR-limit}^2 v_{eigen} v_{max}$ was defined as the amount of thermal energy per unit volume and v in the spherical space. Then, $P' + P'_{eigen}$ of IR energy in 3D was expressed as $3VA_{IR}^2 v_T^2/2$ (Eq. (103)).	Thus, $p' = 12\pi^2 k_{Aq}^2 q^2 A_{IR-limit}^2 v_{eigen} v_{max}$ was defined as the amount of thermal energy per unit volume and v in the spherical space. Then, $P' + P'_{eigen}$ of IR energy in 3D was expressed as $6\pi^2 V k_{Aq}^2 q^2 A_{IR}^2 v_T^2$ (Eq. (103)).
11th page, right, 7th – 10th and the end of Section 11.3.	When $\psi'_{c0-ap2} = 27.8\ \mathrm{m^3/W} = 1/\lambda_t$, conductivity $\lambda_t = 0.036\ \mathrm{W/m^3}$, and $r_1 = 0.1$ m, $K_A = 1.2 \times 10^{-12}$ was obtained using the value of v_{eigen} in the table in Fig. 45.	When $\lambda'_c + \lambda'_r = 0.5$, $k_{Aq} q K_A = 1.97 \times 10^{-18}$ was obtained using the value of v_{eigen} in the table in Fig. 45. ・・・. Based on K_A in Eq. (108), the IR amplitudes included ε_0 and were reduced by $\lambda'_c + \lambda'_r$. The IR energy incorporated ε_0 as permittivity owing to the IR propagation in a vacuum state, making k_ψ smaller than relative permittivity ε_r. ψ_{c0} produced the basic field resisting electrical charge vibration because permittivity represented the degree of influence from electrical field.
11th page, right, the end of Section 12.1.		Incidentally, the lamination structure of $\Delta\theta$ in the θ distribution came from the establishment of the addition theorem of P' in the limited field of an object.

Position	Before Correction	After Correction
11th page, right, Fig.44.	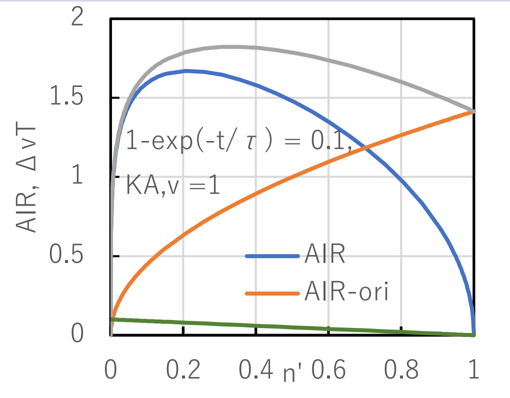 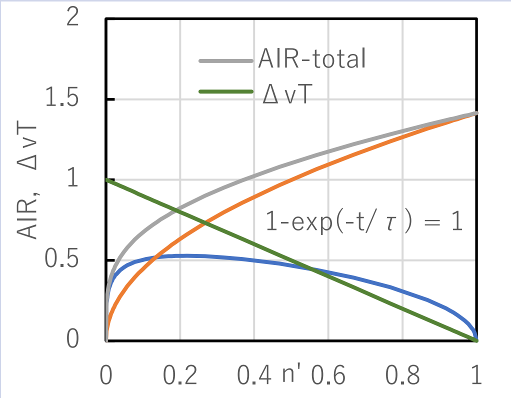	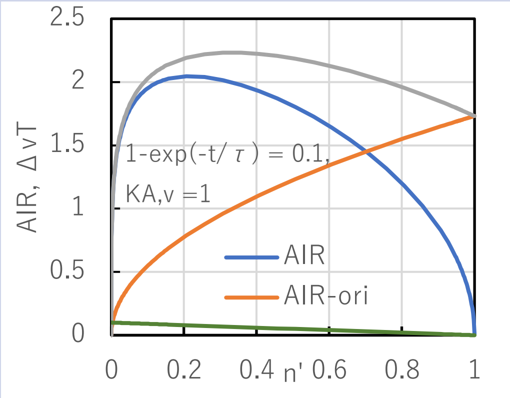 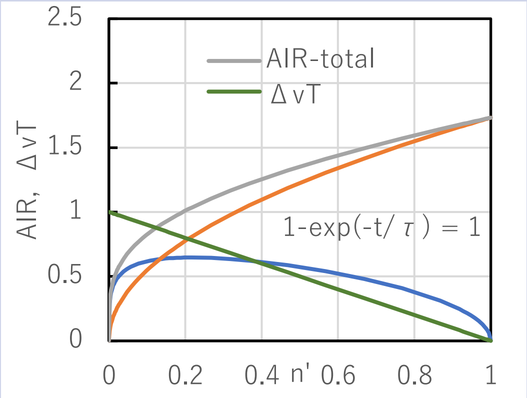
12th page, left, 26th line from bottom.	$\lvert v_{eigen-f}\rvert$ and P'_{eigen} were calculated by the $c\rho_{mol}$ equation in Eq. (117) and $P'_{eigen} = \lvert v_{eigen-f}\rvert h' c\rho_{mol}/2$,	$\lvert v_{eigen-f}\rvert$ and P'_{eigen} were calculated by the $c\rho_{mol}$ equation and $P'_{eigen} = \lvert v_{eigen-f}\rvert h' c\rho_{mol}/2$,
12th page, left, 8th – 12th lines from the bottom.	Hence, the origin A_{IR} was defined by IRs from an ion (Eq. (119)). The A_{IR} of the actual IRs comprised the origin A_{IR} accumulated by the other IRs with the same v_T, according to the theorem of addition for waves.	Hence, the origin A_{IR} defined by IRs from an ion was a constant because of steady $c\rho_{mol}$ (Eq. (119)). Incidentally, Δv_T which was not related to mass and valence was reported, as shown in Eq. (48) and Section 6.2 of the paper (1).
12th page, right, Eqs. (117) – (119).	$\Delta E \approx 12\pi^2 M A_{eigen}^2 v_{eigen} \Delta v_T$ $\Delta E_{IR} \approx 6A_{IR}^2 v_{eigen} \Delta v_T$ $\left(c\rho_{mol} \approx \frac{12\pi^2 N_A M A_{eigen}^2 v_{eigen}}{h'}, \quad v_{eigen} = \lvert v_{eigen-f}\rvert + v_{T0}, \quad P'_{eigen} = 3A_{IR}^2 v_{eigen}^2 = 6\pi^2 M A_{eigen}^2 v_{eigen}^2 \right)$ (117) $E_{IR} \approx 6A_{IR}^2 v_{eigen} \Delta v_T + 3A_{IR}^2 v_{eigen}^2$ (118) $A_{IR} = A_{eigen}\pi\sqrt{2M}$ (119)	$\Delta E \approx 12\pi^2 M A_{eigen}^2 v_{eigen} \Delta v_T \quad (v_{eigen} = \lvert v_{eigen-f}\rvert + v_{T0})$ $\Delta E_{IR} \approx 12\pi^2 k_{Aq}^2 q^2 A_{IR}^2 v_{eigen} \Delta v_T$ $(P'_{eigen} = 6\pi^2 k_{Aq}^2 q^2 A_{IR}^2 v_{eigen}^2)$ ($c\rho_{mol}$ equation was eliminated) (117) $E_{IR} \approx 12\pi^2 k_{Aq}^2 q^2 A_{IR}^2 v_{eigen} \Delta v_T + 6\pi^2 k_{Aq}^2 q^2 A_{IR}^2 v_{eigen}^2$ (118) $k_{Aq} q A_{IR} = A_{eigen}\sqrt{M}$: constant (119)

<table>
<tr><th>Position</th><th>Before Correction</th><th>After Correction</th></tr>
<tr><td>12th page, right, Fig. 45.</td><td>Intercept veigen in IR-class (small)
Presence of negative vT</td><td>Intercept veigen in IR-class (small) : v_{T0}
Presence of negative vT : $v_{eigen-f}$</td></tr>
<tr><td>12th page, right, the end of Section 13.2.</td><td></td><td>

13.3 Consistency of IR energy The mass of the space was negligible, so space alone did not generate SHM. Instead, space vibrations were caused by ion vibrations due to polarization effects. The Coulomb power generated by polarization linked the ion to space, involving q^2 (Fig. 47). Consequently, the ion vibrated in $M(1+\beta_{ir})$, where $\beta_{ir} \propto q^2$. Therefore, the energy of space vibrations was given by: $E_{IR} = 3\beta_{ir}MA_i^2\omega^2/2 = 3k_{Aq}^2q^2A_{IR}^2\omega^2/2$, where k_{Aq} is the factor connecting space to ion. According to Maxwell's equations, the electrostatic field energy was $I = \varepsilon_0 E_f^2/2$. For IR energy, the electric field E_f depended on the charge q and A_{IR}. However, for example, E_f for $A_{IR\text{-}ori}$ in Eq. (12) did not incorporate q (Eq. (120)). Thus, in the context of τ, IRs were unrelated to valence. $E_{IR}/(4\pi r^2)^2$ corresponding to I came from $k_{Aq}qA_{IR}/(4\pi r^2)$ that qA_{IR} distributed in all directions was divided by surface area.

$$E_f = \frac{1}{16\pi^3 r_1^3 r^2}\sqrt{\frac{3h\prime(1-\lambda\prime_c-\lambda\prime_r)}{v_{eigen}}} \qquad \left(\frac{E_{IR}}{(4\pi r^2)^2} = \frac{3\varepsilon_0 E_f^2\omega_T^2}{2}, k_\psi = 1\right) \qquad (120)$$

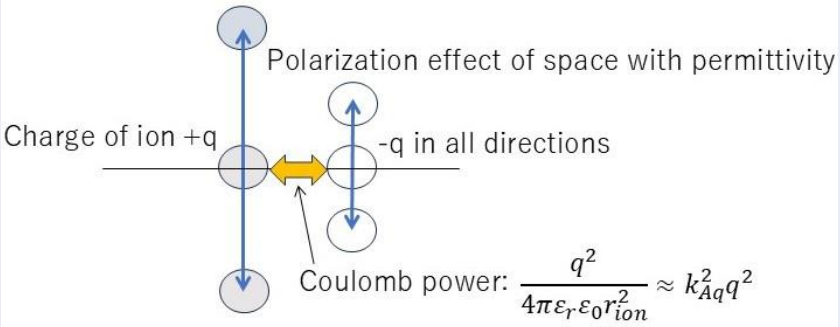

Fig. 47 Connection with Coulomb power.
</td></tr>
</table>

Position	Before Correction	After Correction
13th page, left, 32th line from top.	The electrical potential energy of finite value at $r = 0$ was studied for ions. The steady amplitude of ion vibration that was steadied under a high slope of V_p was verified ・・・. Additionally, ・・・ because it was found that motions other ・・・	The amplitude of ion vibration that was steadied under a high slope of V_p was verified ・・・. Additionally, ・・・ because it was found that, SHM resonated with spin having fixed r_t, the SHM amplitude was characterized by changeableness, and, motions other ・・・
13th page, Appendix, 1. Before correction.		(Addition) **1.8 Fifth page, right, 9th from the top** In this manner, the high thermal insulation property was obtained. **1.9 Fifth page, left, figure 11** 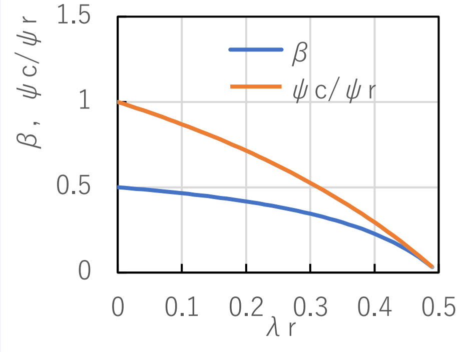 Fig. 11 Trends of β and ψ_c/ψ_r. **1.10 Sixth page, left, first line from top** direction, as shown in Fig. 13. **1.11 Sixth page, right, equation (42)** $\left(K_{red} = 12\pi^2\beta_{ir}MA_i{}^2v_{eigen}, IR_{ori} < 6\pi^2M_eA_i^2v_T^2\right)$ **1.12 Seventh page, left, 7th line from bottom** Here, the E_{fA} of the dent took a finite value with the distance r_{dent}. **1.13 Seventh page, right, second line from top** however, its curve was nearly flat to be the exponent 1/3. **1.14 Seventh page, right, equation (49)** $f_{resilience} = q\frac{dV_{pAB}}{dt} = q\frac{d(V_{pB}-V_{pA})}{dt}$ (Next item numbers are moved up.)

Position	Before Correction	After Correction
14th page, Appendix, 2. After correction.		(Addition) **2.8 Fifth page, right, 9th from the top** In this manner, the high thermal insulation property was obtained, as shown in Fig. 31. **2.9 Fifth page, left, figure 11** 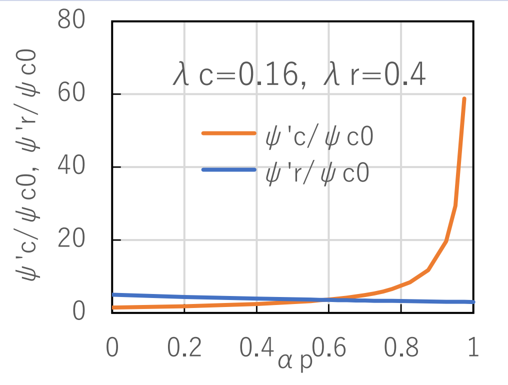 Fig. 11 Trends of ψ'_c/ψ_{c0} and ψ'_r/ψ_{c0} . **2.10 Sixth page, left, first line from top** 3 D, as shown in Fig. 13. **2.11 Sixth page, right, equation (42)** $\left(\begin{matrix} K_{red} = 12\pi^2 \beta_{ir} M {A_i}^2 v_{eigen}, IR_{ori} < 6\pi^2 M_e A_i^2 v_T^2, \\ \beta_{ir} = \frac{3h\prime m(1-\lambda_c-\lambda_r)}{16\pi^4 r_1^6 M {A_i}^2 v_{eigen} k_\psi \varepsilon_0} \end{matrix}\right)$ **2.12 Seventh page, left, 7th line from bottom** Here, the E_{fA} of the dent took a finite value with r_{dent}, as shown in Fig. 22. **2.13 Seventh page, right, second line from top** however, its curve was nearly flat to be the exponent 1/3, as shown in Fig. 25. **2.14 Seventh page, right, equation (49)** $f_{resilence} = q\frac{dV_{pAB}}{dr} = q\frac{d(V_{pB}-V_{pA})}{dr}$ (Next item numbers are moved up.)